

# Nuclear Matter Calculations and Phenomenological Potentials\*

K. A. BRUECKNER†

*Institute for Defense Analyses, Washington, D. C.*

AND

K. S. MASTERSON, JR.‡

*University of California, San Diego, La Jolla, California*

(Received June 18, 1962)

The properties of nuclear matter predicted for several different phenomenological potentials by the reaction matrix theory of Brueckner have been calculated. The calculations have shown that potentials which give supposedly equally good fit to scattering data do not necessarily lead to identical nuclear properties. Other approximation methods have been studied to determine their accuracy, with particular emphasis on the iterated Born approximation, and on comparison with the Moszkowski-Scott separation method and with the approximations of Mohling and of Puff.

## I. INTRODUCTION

IN a series of previous papers,<sup>1</sup> methods have been developed for the determination of the properties of nuclear matter. This theory has been applied by Brueckner and Gammel<sup>1</sup> (hereafter referred to as BG) to extended nuclear matter using both Gammel-Christian-Thaler potentials<sup>2</sup> and one of the sets of Gammel-Thaler potentials.<sup>3,4</sup> The latter were modified slightly to give correctly the low-energy scattering parameters and deuteron properties. Accurate numerical solutions of the equations of the theory gave a mean binding energy of  $-15.2$  MeV and equilibrium spacing of  $1.02$  F for the modified Gammel-Thaler potentials, in good agreement with semiempirical values for the binding energy ranging from  $-15.83$  MeV reported by Green<sup>5</sup> to  $-17.04$  MeV obtained by Cameron,<sup>6</sup> and with the equilibrium spacing,  $r_0 = (1.07 \pm 0.02)$  deduced from high-energy electron-nucleus scattering.

A detailed discussion of the  $K$ -matrix theory and the method of applying it to extended nuclear matter is contained in BG. Consequently, we shall indicate here only the basic equations, and in the next section introduce our additional approximations.

In BG, the  $K$  matrix from which the energy is computed is defined by the equation

$$K_{ij,kl} = V_{ij,kl} + \sum_{\substack{m,n \\ p_m > p_F \\ p_n > p_F}} V_{ij,mn} \frac{1}{E_k + E_l - E_m^* - E_n^*} K_{mn,kl}. \quad (1.1)$$

In this equation  $E_k$  and  $E_l$  are self-consistent energies for particles moving in the Fermi gas and  $E_m^*$  and  $E_n^*$  are energies appropriate to virtual excitations above the Fermi surface. The single-particle potential is determined from the diagonal elements of the  $K$  matrix by the relation

$$V(p_i) = \sum_j (K_{ij,ij} - K_{ij,ji}) \quad (1.2)$$

with the sum over all filled states. Finally, the average binding energy per particle is

$$E_{av} = \frac{3}{p_F^3} \int_0^{p_F} p^2 dp \left[ \frac{p^2}{2m} + \frac{1}{2} V(p) \right]. \quad (1.3)$$

The normal density is assumed to be determined from the minimum of  $E_{av}$  as a function of density.

In the present paper we use an approximation of the Brueckner formalism which is simpler than that used in BG,

(1) to investigate the properties of nuclear matter predicted by the theory for various phenomenological potentials (six Gammel-Thaler potentials<sup>7</sup> and the Breit potential<sup>8</sup>);

(2) to check the rapidity of convergence of successive Born approximations;

(3) to obtain a comparison with the results of the separation method of Moszkowski and Scott<sup>9,10</sup>; and

(4) to check the accuracy of the approximation described by Bell<sup>11</sup> as the central element in the nuclear matter theories of Mohling<sup>12</sup> and of Puff and Martin.<sup>13</sup>

\* This work was done in part under the auspices of the U. S. Atomic Energy Commission.

† Permanent address: University of California, San Diego, La Jolla, California.

‡ Lieutenant, U. S. Navy, on duty under instruction at the University of California.

<sup>1</sup> See K. A. Brueckner and J. L. Gammel, Phys. Rev. **109**, 1023 (1958), for a list of references.

<sup>2</sup> J. L. Gammel, R. S. Christian, and R. M. Thaler, Phys. Rev. **105**, 311 (1957).

<sup>3</sup> J. Gammel and R. M. Thaler, Phys. Rev. **107**, 291 (1957).

<sup>4</sup> J. Gammel and R. M. Thaler, Phys. Rev. **107**, 1337 (1957).

<sup>5</sup> A. E. S. Green, Revs. Modern Phys. **30**, 569 (1958); Phys. Rev. **95**, 1006 (1954).

<sup>6</sup> A. G. W. Cameron, Can. J. Phys. **35**, 1021 (1957).

<sup>7</sup> J. S. Gammel and R. M. Thaler, in *Progress in Elementary and Cosmic Ray Physics*, edited by J. G. Wilson and S. A. Wouthuysen (North-Holland Publishing Company, Amsterdam, 1960), Vol. V, Chap. 11.

<sup>8</sup> K. E. Lassila, M. H. Hull, Jr., H. M. Ruppel, F. A. McDonald, and G. Breit, Phys. Rev. **126**, 881 (1962).

<sup>9</sup> S. A. Moszkowski and B. L. Scott, Ann. Phys. (New York) **11**, 65 (1960).

<sup>10</sup> B. L. Scott and S. A. Moszkowski, Ann. Phys. (New York) **14**, 107 (1961).

<sup>11</sup> J. S. Bell, in *Proceedings of the Rutherford Jubilee International Conference* (Heywood & Co., London, 1961), p. 373.

<sup>12</sup> F. Mohling, Phys. Rev. **124**, 583 (1961).

<sup>13</sup> P. C. Martin and J. Schwinger, Phys. Rev. **115**, 1342 (1959); R. D. Puff and P. C. Martin, Bull. Am. Phys. Soc. **5**, 30 (1960); R. D. Puff, Ann. Phys. (New York) **13**, 317 (1961).

## II. SOLUTION OF THE K-MATRIX EQUATIONS

In the investigations reported in this paper, we used the procedure of BG with one further approximation: We have assumed that the difference of energies in the denominator of Eq. (1.1) is independent of the total momentum. Thus, we make the replacement

$$E_k + E_l - E_m^* - E_n^* = 2[E(p_{kl}) - E^*(p_{mn})], \quad (2.1)$$

with  $p_{kl}$  and  $p_{mn}$  the relative momenta. This approximation is accurate if  $E_k$  has a quadratic dependence on  $p_k$  or if the relative momentum is large compared with the total momentum. Consistent with the accuracy of this approximation, we replace the total momentum, which enters in the treatment of the exclusion principle, by its average value compatible with a given value of relative momentum,  $k$ . This is easily shown to be

$$\left(\frac{P^2}{4}\right)_{av} = \frac{\frac{3}{5}p_F^2 \left(1 - \frac{k}{p_F}\right) \left(1 + \frac{1}{2}k/p_F + \frac{1}{6}k^2/p_F^2\right)}{\left(1 + \frac{1}{2}k/p_F\right)}, \quad k < k_F. \quad (2.2)$$

For  $k \geq p_F$ , we have set  $P_{av} = 0$ . These simplifications reduce considerably the problem of solving the BG

equations and are not thought to introduce appreciable errors into the results, particularly since we are primarily interested in comparisons among various potentials and approximation methods.

We quote here the principal equations to be solved, as adapted from BG:

(1) Green's functions:

$$G_l(r, r') = \frac{1}{2\pi^2} \int_0^\infty \frac{k'^2 dk'' j_l(k''r) j_l(k''r') f(P, k'')}{2[E(k) - E^*(k'')]}. \quad (2.3)$$

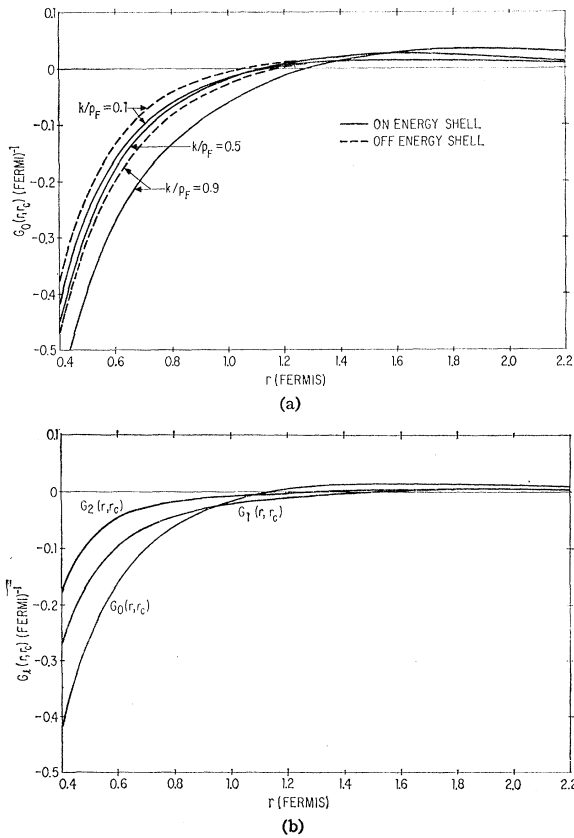


FIG. 1. Green's functions for BGT potential at  $r_0=1.00$  F: (a)  $G_0(r, r_c)$  for several values of  $k/p_F$ , both on- and off-energy shell; (b)  $G_l(r, r_c)$  for  $l=0, 1$ , and  $2$ , and for  $k/p_F=0.1$  on-energy shell. The BGT potential is the one used by Brueckner and Gammel (reference 1).

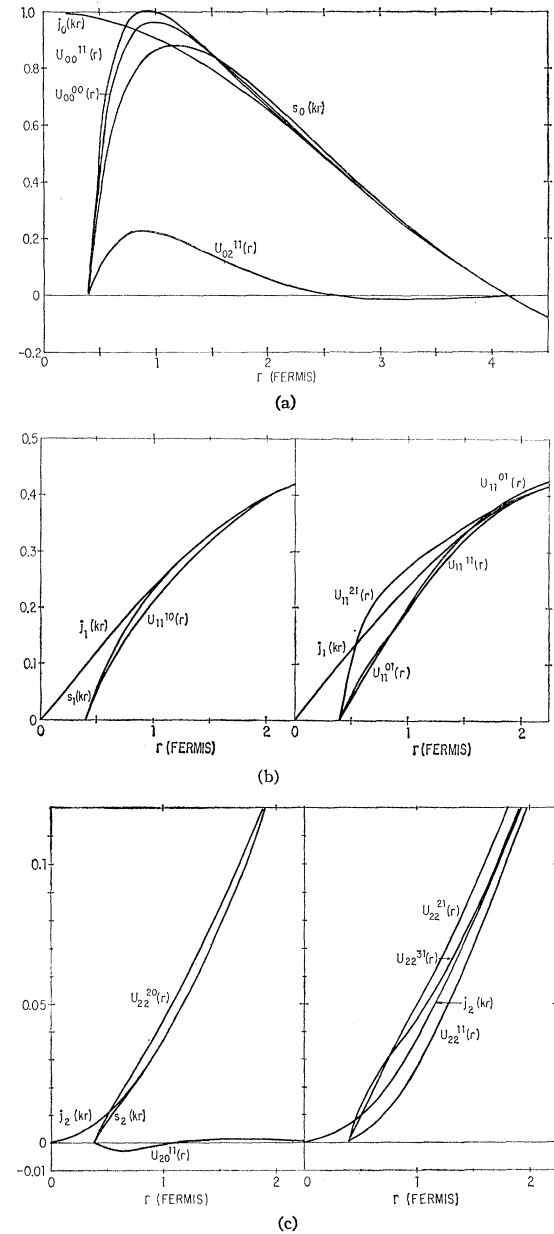


FIG. 2. Wave functions for BGT potential at  $r_0=1.00$  F: (a) for  $k/p_F=0.5$  and  $l=0$ ; (b) for  $k/p_F=0.5$  and  $l=1$ ; (c) for  $k/p_F=0.5$  and  $l=2$ .

for on-energy-shell propagation, and with  $\{2[E(k) - E^*(k'')] - \Delta\}$  in the denominator for off-energy-shell propagation (see Fig. 1).  $\Delta$  is the mean excitation energy, assumed to be  $E(p_F) - E(0)$ . The Pauli step function,  $f(P, k'')$ , is that given in BG Eq. (34) with the total momentum  $P$  replaced by  $P_{av}$  of Eq. (2.2); it excludes from the integrand values of  $k''$  not allowed by the exclusion principle.

(2) Plane wave basis functions and Green's functions as modified by the hard-core potential of radius  $r_c$ :

$$s_l(kr) = j_l(kr) - [j_l(kr_c)G_l(r, r_c)/G_l(r_c, r_c)], \quad (2.4)$$

$$F_l(r, r') = G_l(r, r') - [G_l(r, r_c)G_l(r_c, r')/G_l(r_c, r_c)]. \quad (2.5)$$

As shown in BG, the above definitions result from requiring the wave functions (next equation) to vanish at the core (see Fig. 2).

(3) Wave functions:

$$U_{l'J^s}(k, r) = s_l(kr)\delta_{ll'} + 4\pi \sum_{l''} \int_{r_c}^{\infty} r'^2 dr' F_{l''}(r, r') V_{l'l''J^s}(r') U_{l'J^s}(r'), \quad (2.6)$$

where the  $V_{l'l''J^s}(r')$  are the phenomenological two-body potentials.

(4)  $K$  matrices:

$$(k|K|k) = \sum_{J_s} \sum_{l=J-1}^{J+1} C_{Jls} \left\{ -\frac{j_l^2(kr_c)}{G_l(r_c, r_c)} + 4\pi \int_{r_c}^{\infty} r^2 dr s_l(kr) \sum_{l'=J-1}^{J+1} V_{ll'J^s}(r) U_{l'J^s}(r) \right\}, \quad (2.7)$$

where  $C_{Jls}$  is the appropriate statistical weight, and  $s$  is the spin index (see Fig. 3).

(5) Single-particle potential:

$$V(p) = \frac{6}{\pi^2} \int_0^{(p_F-p)/2} k'^2 dk' (k'|K|k') + \frac{3}{\pi^2} \int_{|p_F-p|/2}^{(p_F+p)/2} k'^2 dk' (k'|K|k') \times \left( 1 + \frac{p_F^2 - p^2 - 4k'^2}{4pk'} \right), \quad (2.8)$$

for  $p < p_F$ . For  $p \geq p_F$ , the first integral vanishes (see Fig. 4).

### III. COMPUTATIONAL PROCEDURE

The computations were performed on the CDC-1604 solid-state digital computer. The compiler used was

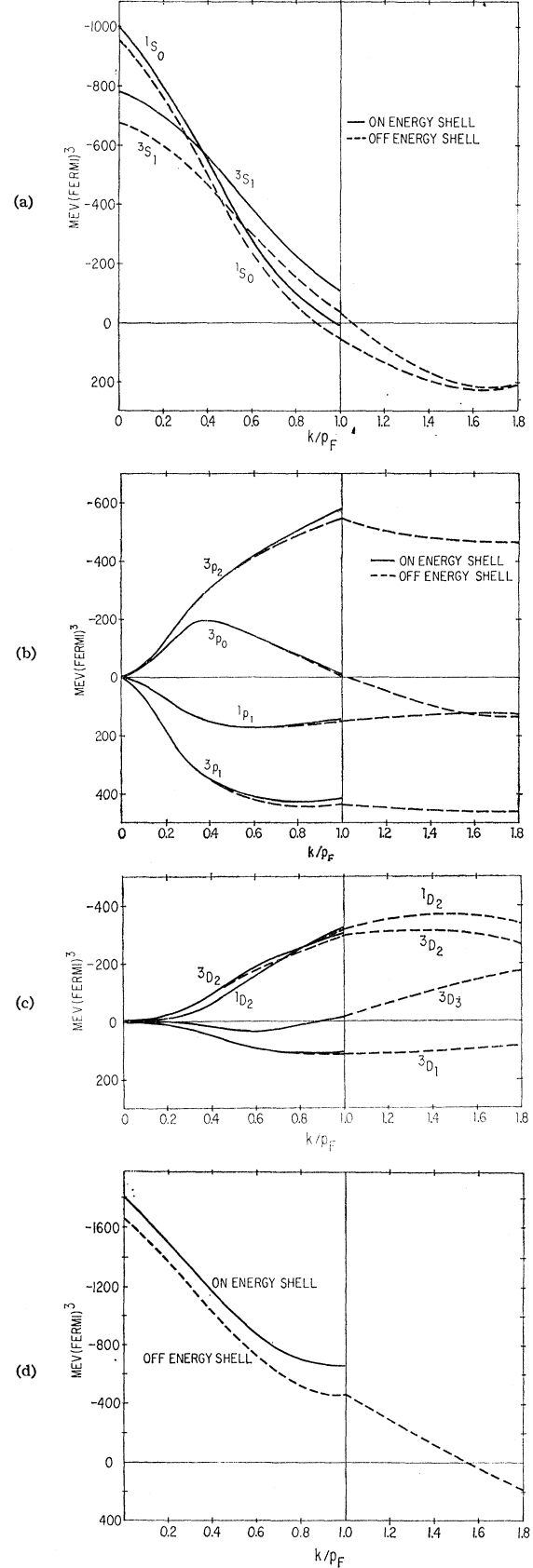


FIG. 3. Diagonal elements of the  $K$  matrix for BGT potential at  $r_0 = 1.00$  F: (a)  $S$  states; (b)  $P$  states; (c)  $D$  states; (d) total. Statistical weights are included.

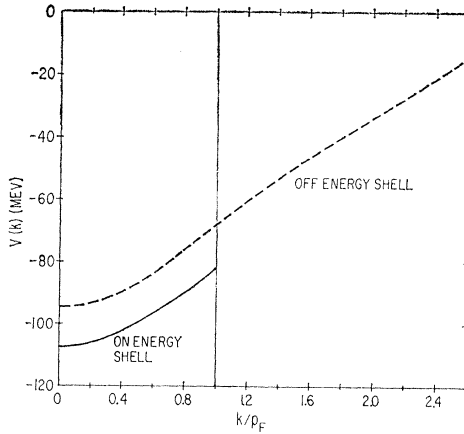


FIG. 4. Self-consistent single-particle potential  $V(k)$  for BGT potential at  $r_0 = 1.00$  F.

NELIAC,<sup>14</sup> and initial compilation and debugging was done on a Burroughs 220 at the U. S. Navy Electronics Laboratory, San Diego, California. Subsequently the problem was transferred to the computer at the University of California at San Diego, on which final debugging and production runs were made.

The computational procedure was straightforward. The Green's functions [Eqs. (2.3) and (2.5)] were first computed. The first approximation for the energies appearing in the denominators was

$$\begin{aligned} E(k) &= k^2/2M, & k < p_F \\ &= p_F^2/2M, & k \geq p_F; \\ E^*(k'') &= k''^2/2M, & \text{all } k''. \end{aligned} \quad (3.1)$$

The integration was done numerically to an intermediate value of  $k$ ,  $k_{\text{int}}$ , and the integral from  $k_{\text{int}}$  to infinity was replaced by an analytical approximation to the following integral:

$$-\frac{M}{2\pi^2} \int_{k_{\text{int}}}^{\infty} j_l(k''r) j_l(k''r') dk''. \quad (3.2)$$

Here we have assumed that  $E(k) \ll E^*(k'' \geq k_{\text{int}})$  and  $E^*(k'' \geq k_{\text{int}}) = k''^2/2M$ . On subsequent iterations, for  $k \leq 2.6p_F$ , values of  $E(k)$  and  $E^*(k'')$  from the previous iteration were used in place of Eq. (4.1) [with  $E(k > p_F) = E(p_F)$ ]. For  $k'' > 2.6p_F$  we use (as in BG)

$$E^*(k'' > 2.6p_F) = k''^2/2M. \quad (3.3)$$

Each cycle leading to a new table of  $E(k)$  and  $E^*(k'')$  is called a major iteration.

The wave functions were then computed by iteration of Eq. (2.6). On the first iteration, the  $s_l(kr)$  [Eq. (2.4)] were used as the first guess. On subsequent major iterations, the wave function from the previous iteration

was used as the first guess. Each wave function iteration took about one second (for  $S$ ,  $P$ , and  $D$  waves).

The  $K$ -matrix elements [Eq. (2.7)] were computed by numerical integration from  $r=r_{\text{core}}$  to  $r=r_{\text{max}}$ , where  $r_{\text{max}}$  was chosen such that contributions to the integral from higher terms were negligible (the exponential behavior of the  $V_{ll'} J^s(r)$  made this possible).

The potential energies [Eq. (2.8)] were then computed by numerical integration and the new energy table was formed, with

$$E(k) = (k^2/2M) + V(p=k). \quad (3.4)$$

The binding energy was then computed from Eq. (1.3), completing the major iteration. Four minutes were required for a major iteration if the wave functions were iterated five times.

In the computations, all of the meshes used for the numerical integrations could be varied. In addition, in several cases both Weddle's rule and Simpson's rule could be employed for the first seven points. Simpson's rule was found to be adequate in all cases, and was employed in the calculations reported.

The following meshes (in fermis or inverse fermis) yielded agreement of calculated binding energy to within 0.1 MeV of the most accurate results obtainable with our code:

(1) Green's functions [Eq. (2.3)] and wave functions [Eq. (2.6)]:

$$\begin{aligned} r, r' &= 0.4(0.05)0.7(0.1)1.5(0.2)2.3(0.5)4.3 \text{ (F)}, \\ k'' &= 0(0.05)10 \text{ (F}^{-1}\text{)} \text{ for } G_l(r_c, r_c) \\ &= 0(0.2)10 \text{ (F}^{-1}\text{)} \text{ otherwise.} \end{aligned} \quad (3.5)$$

The additional precision for  $G_l(r_c, r_c)$  was desired because of its importance in the modified Green's functions [Eq. (2.5)] and in the core term in the  $K$ -matrix equation [Eq. (2.7)].

(2)  $K$ -matrix elements [Eq. (2.7)]:

$$r, r' = 0.4(0.05)0.7(0.1)1.5(0.2)2.3(0.5)8.3 \text{ (F)}, \quad (3.6)$$

with

$$U_{ll'} J^s(kr > 4.3k) = \delta_{ll'} j_l(kr), \quad (3.7)$$

for the following values of  $k$ :

$$\begin{aligned} k &= 0.1(0.2)0.9p_F \text{ on- and off-energy shell} \\ &= 1.0(0.4)1.8p_F \text{ off-energy shell.} \end{aligned} \quad (3.8)$$

(3) Potential energies [Eq. (2.8)] and self-consistent total energies:

$$\begin{aligned} k' &= 0(0.05)1.8p_F, \\ p &= 0(0.2)2.6p_F. \end{aligned} \quad (3.9)$$

(4) Mean binding energy [Eq. (1.3)]:

$$p = 0(0.05)1.0p_F. \quad (3.10)$$

The  $K$  matrix and energy tables were interpolated quadratically as necessary.

<sup>14</sup> H. Huskey, M. H. Halstead, and R. McArthur, Communications of the Association for Computing Machinery **3**, 463 (1960); K. S. Masterson, Jr., *ibid.* **3**, 608 (1960).

TABLE I. Parameters of the Gammel-Thaler potentials (reference 7). BGT is the potential used by Brueckner and Gammel.<sup>a</sup>  $r_0=0.40$  F except as indicated. Triplet and singlet states are designated by 3 and 1, respectively, and parity by + and -. As explained in text, BGT odd-state potentials were used instead of the GT odd-state potentials in all calculations where not otherwise indicated.

Potential	${}^3V_{\sigma}^+$ (MeV)	${}^3\mu_{\sigma}^+$ (fermi) <sup>-1</sup>	${}^3V_{T^+}$ (MeV)	${}^3\mu_{T^+}$ (fermi) <sup>-1</sup>	${}^3V_{LS^+}$ (MeV)	${}^3\mu_{LS^+}$ (fermi) <sup>-1</sup>	${}^1V_{\sigma}^+$ (MeV)	${}^1\mu_{\sigma}^+$ (fermi) <sup>-1</sup>
4100	-87.724	1.2183	-272.87	1.2183	0	...	-425.5	1.450
4200	-726.69	1.9554	-121.04	0.97772	0	...	-425.5	1.450
4205	-877.39	2.0909	-159.46	1.0454	-5000	3.7	-425.5	1.450
BGT	-877.4	2.091	-159.4	1.045	-5000	3.7	-434	1.450
4305	-1964.4	2.4247	-67.106	0.80823	-5000	3.7	-425.5	1.450
4400	-2019.9	2.3259	-22.719	0.58147	0	...	-425.5	1.450
	${}^3V_{\sigma}^-$	${}^3\mu_{\sigma}^-$	${}^3V_{T^-}$	${}^3\mu_{T^-}$	${}^3V_{LS^-}$	${}^3\mu_{LS^-}$	${}^1V_{\sigma}^-$	${}^1\mu_{\sigma}^-$
BGT	-14.0	1.00	22.0	0.80	-7315	3.7	130.0	1.0
All others	0	...	22.0 <sup>b</sup>	0.80	-7317.5 <sup>b</sup>	3.7	70	1.0

<sup>a</sup> See reference 1.

<sup>b</sup>  $r_0=0.4125$  F.

The normal computation procedure was to compute Green's functions, wave functions, and  $K$ -matrix elements for each value of  $k$ , and to do the energy computations after all the  $K$ -matrix elements had been computed.

In order to investigate the rate of convergence of successive Born approximations and to evaluate the rate of convergence of the wave-function iteration procedure, the code was designed so that  $K$  matrices could be calculated after each wave function iteration, and from these the binding energy was computed. Two procedures for iterating the wave functions were employed. In order to obtain the successive Born approximations, two tables of wave functions were used. The "old" table was used on the right side of Eq. (2.6) to generate a "new" table [the left side of Eq. (2.6)]. In order to increase the rate of convergence, the two wave-functions tables were replaced for the remainder of the calculations by a single table, and the integration was performed with the same table used for both sides of Eq. (2.6). In addition, instead of starting each major iteration with

$$U_{ll'}^{J^s}(r) = \delta_{ll'} s_l(kr) \quad (3.11)$$

as the initial value for the right side of Eq. (2.6), as was done for the Born approximations, we saved the wave functions from the previous major iteration as the "first guess" in the subsequent major iteration.

The above procedure was used for angular momentum states with  $l=0, 1$ , and  $2$ . The contribution from higher states has been previously shown to be negligible.<sup>1</sup>

#### IV. RESULTS

##### A. Application to the Gammel-Thaler and Breit Potentials

As a check on the method, we first determined the energy and equilibrium density of nuclear matter using the Brueckner-Gammel-Thaler (BGT) potential previously used by BG. The result was a binding energy of  $-16.9$  MeV at  $r_0=1.00$  F, compared to the BG values of  $-15.2$  MeV at  $r_0=1.02$  F. This difference gives a

measure of the error introduced by the approximations of this paper. In Figs. 1 through 4 we present some of the intermediate quantities computed (Green's functions, modified basis functions, wave functions,  $K$  matrices, and self-consistent single-particle potential) for the BGT potential with  $r_0=1.00$  F ( $p_F=1.52$  F<sup>-1</sup>).

To determine the variation of nuclear properties with various phenomenological potentials, we have calculated energy and equilibrium density for a set of Gammel-Thaler (GT) potentials and for the Breit potential. The Gammel-Thaler potentials differ from each other primarily in the central-tensor force ratio and the magnitude of spin-orbit force in the triplet even states. They give equally good fit to the binding energy and electric quadrupole moment of the deuteron and to the triplet neutron-proton scattering length, as well as good fits to scattering data up to about 90 MeV. Their parameters are given in Table I. Except where otherwise noted, the BGT odd state potentials were used in place of the GT odd state potentials because of a different core in the latter. This substitution was checked and was found to introduce negligible error.

The Breit potential is of the form

$$V = V^{(2)} + V_{\sigma} + V_T S_{12} + V_{LS}(\mathbf{L} \cdot \mathbf{S}) + V_{\sigma}[Q_{12} - (\mathbf{L} \cdot \mathbf{S})^2]. \quad (4.1)$$

The operator  $[Q_{12} - (\mathbf{L} \cdot \mathbf{S})^2]$  has the value  $-L(L+1)$  for uncoupled states,  $J=L$ , and is zero otherwise.  $V^{(2)}$  is the one-pion-exchange potential,

$$V^{(2)} = \frac{1}{3} \mu_{\pi} \boldsymbol{\tau}^{(1)} \cdot \boldsymbol{\tau}^{(2)} \times \frac{f^2}{4\pi} \left\{ \left[ \boldsymbol{\sigma}^{(1)} \cdot \boldsymbol{\sigma}^{(2)} + S_{12} \left( 1 + \frac{3}{x} + \frac{3}{x^2} \right) \right] \frac{e^{-x}}{x} + \boldsymbol{\sigma}^{(1)} \cdot \boldsymbol{\sigma}^{(2)} \delta(x) \right\}, \quad (4.2)$$

where  $\mu_{\pi}$  is the pion mass, and  $x = \mu_{\pi} r$  (in units where  $c = \hbar = 1$ ). The delta-function term can be neglected in actual computations. The coupling constant,  $f^2$ , is

TABLE II. Parameters of the Breit potential (reference 8). Values of coefficients  $a_n$  in Eq. (4.4) are in MeV. Notation same as in Table I.

Potential	$n=0$	1	2	3	4	5	6	7
$^1V_c^+$	21.925	-19.6303	-194.782	66.4334	-15.2873	-14.5395	1.115	0
$^1V_q^+$	0.333	0.5	0.1	-2.0	-5.1083	-0.2333	0.2	0
$^3V_c^-$	0	-14.28	18.72	-17.3	0	-5.3	-1.3	0
$^3V_T^-$	1.5	50.8984	-83.3812	8.7693	-3.1988	1.6172	0.52	0
$^3V_{LS}^-$	0	0	0	0	-2.9794	-76.4565	43.8285	-7.4186
$^1V_c^+$	0	-96.0	-71.001	18.0	8.0	125.8	5.01	0
$^3V_c^+$	0	-47.667	-18.47	-1.00	-3.55	0	0	0
$^3V_T^+$	0	17.3933	7.775	13.535	3.0	-1.4971	0	0
$^3V_{LS}^+$	0	0	0	0	14.35	7.4875	0	0
$^3V_q^+$	0	0	5.3333	0	-13.5917	-7.4167	-1.6667	0

given in terms of the related constant,  $g_0^2$ , by

$$(4\pi)^{-1}f^2 = g_0^2(\mu_\pi/2M)^2 \simeq g_0^2/14^2, \quad (4.3)$$

where  $M$  is the nucleon mass. All the other potentials on the right side of Eq. (4.2) have the form

$$V = \sum_n a_n e^{-2x}/x^n. \quad (4.4)$$

The values of  $a_n$  are listed in Table II. For singlet even states,  $g_0^2/14 = 0.94$ . It is unity otherwise. All potentials have a hard core corresponding to  $x_c = 0.35$ . For singlet-even and triplet-odd states the neutral pion mass is used, and for singlet-odd and triplet-even states a weighted mean of charged and neutral pion masses is used in the proportion of two to one. With  $\mu_{\pi_0} = 135$  MeV and  $\mu_{\pi^\pm} = 139.59$  MeV, this has the effect of requiring two core radii, 0.5116 F for the first and 0.5002 F for the second group of states.

Curves of binding energy vs  $r_0$  for the Gammel-Thaler and the Breit potentials are given in Fig. 5. The binding energy and equilibrium spacing for these potentials are given in Table III. We also include in this table the

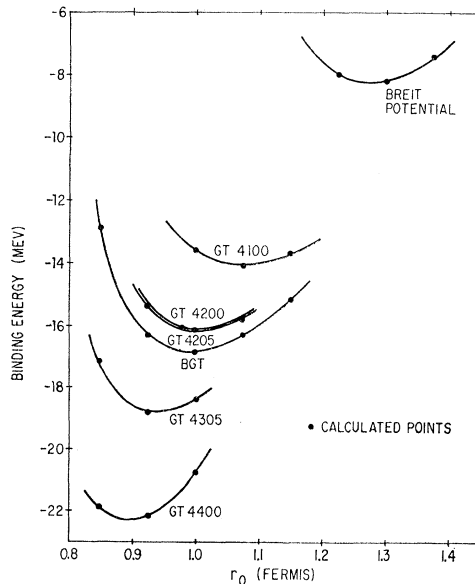


FIG. 5. Binding energy vs  $r_0$  for the phenomenological potentials of Tables I and II.

binding energy for the various potentials at  $r_0 = 1.00$  F, including the effect of some modifications to the Breit potential and (for comparison) to the BGT potential.

These results for the Gammel-Thaler potentials show the considerable sensitivity of the binding energy and density to the central-tensor force admixture of the Gammel-Thaler potentials, the energy varying from -14.1 to -22.3 MeV and the spacing from 0.90 to 1.08 F. The potentials with stronger central forces give greater binding at higher density. The results also indicate that the even-spin-orbit force has negligible effect.

The results obtained for the Breit potential show even more sensitivity to the potential form, since the binding energy -8.3 MeV at a spacing of 1.28 F is quite far from the empirical value. The considerable difference between the results of the Gammel-Thaler and Breit potentials appears to be due to these features of the Breit potential: (a) larger core radius, (b) strong odd-state repulsion, (c) quadratic spin-orbit terms, and (d) weaker even triplet central force. These changes were introduced to give an improved fit to high-energy scattering data and to match the one-meson-exchange potential at large separation. Breit and his co-workers point out, however, that this potential is not unique, and that several features of the potential were to some extent arbitrary. It is also probable that the condition of matching the meson potential should not be literally interpreted for distances inside 2 or 3 F. If this condition is altered, a weaker even-state tensor force could be used, with a corresponding increase in the even triplet central force. The results of the calculations of the present paper point clearly to the need for further investigation with the goal of determining a truly unique potential.

### B. Convergence of Successive Approximations

Equation (1.1) for the  $K$  matrix and Eq. (1.2) for the single-particle potential energy can be solved by successive approximation. It has been suggested that to a good approximation the energy can be obtained from first and second Born approximations applied to the long-ranged part of the interaction after the repulsive core has been separated and treated more exactly.

To study the accuracy of various approximations to Eqs. (1.1) and (1.2), we have first used the procedure of BG to treat the effects of the repulsive core, obtaining the equations quoted in Sec. II. A complete discussion of this treatment can be found in BG.

In solving these equations, we can determine the effects of two types of successive approximations. Since Eq. (2.6) for  $U_{ll}^{J*}(k, r)$  was first solved by iteration starting from  $s_l(kr)$  as the first approximation, it was easy to evaluate the energy for various iterations of the wave function. This we term the first, second, etc., Born approximation, although this term is not strictly correct since we have treated the core exactly.

The second successive approximation is in the evaluation of the Green's function,  $G_l(r, r')$ , Eq. (2.3). We have started in our calculations with the first input for  $E_k$

TABLE III. Binding energy and equilibrium spacing for potentials discussed in paper. Results indicated for modified potentials are calculated with a single-particle potential,  $V(k)$ , self-consistent with respect to the modified potential.

Potential	Minimum binding energy (MeV)	Equilibrium spacing (F)	Binding energy at $r_0=1.00$ F (MeV)
GT 4100	-14.1	1.08	-13.6
GT 4200	-16.1	1.01	-16.1
GT 4205	-16.2	1.01	-16.2
BG			
(a) full	-16.9	1.00	-16.9
(b) without $^3V_T^+$			-2.8
(c) without $P$ states			-18.1
(d) without $P$ -state core			-23.1
GT 4305	-18.8	0.94	-18.4
GT 4400	-22.3	0.90	-20.8
Breit			
(a) full	-8.3	1.28	-0.3
(b) without $P$ states			-9.2
(c) without $P$ states			-12.7
$^3V_T^+$ and $^1V_T^+$			
(d) without $P$ -state core			-14.6
(e) without $P$ and $D$ core			-15.2

simply

$$E(k) = k^2/2M.$$

This we call the first major iteration. In successive major iterations, we determine  $V(k)$  from the previous major iteration for  $(k|K|k)$ .

A typical result for the binding energy as a function of successive Born approximations for the wave function is given in Table IV. The results of successive major iterations for the single-particle energies is given in Table V. These results show that the  $K$  matrix must be computed to at least third order in the interaction and that the self-consistent energy must be determined from  $K$  matrices which themselves have the single particle energies accurate to at least first order in the  $K$  matrices.

The importance of using energies which are self-consistent both as a function of phenomenological potential employed and as a function of  $r_0$  (e.g., of Fermi momentum) is illustrated by the self-consistent

TABLE IV. Illustrative binding energy sequence for successive iterations of the wave function Eq. (2.6). Energies are in MeV.

Major iteration	Born approximation	Binding energy
I	1	+1.304
	2	-19.590
	3	-25.974
	4	-26.824
II	1	+7.578
	2	-8.337
	3	-11.756
	4	-12.022
	5	-12.046
	6	-12.049

potential curves of Fig. 6(a) [in which we show the  $V(k)$  appropriate to several different phenomenological potentials at  $p_F=1.52$  F $^{-1}$  ( $r_0=1.00$  F)], and Fig. 6(b) [in which  $V(k)$  is shown for several values of  $p_F$ ]. To test the dependence of the calculations on  $V(k)$ , we calculated at several densities the binding energy for the BGT potential using the  $V(k)$  which was self-consistent at the energy minimum ( $r_0=1.00$  F). The result, shown in Fig. 7, clearly indicates the importance of the self-consistency requirement; there is no sign of saturation near normal density—the minimum is -23.2 MeV at  $r_0=0.79$  F.

The slow convergence of the Born approximation sequence for the wave function is to a considerable extent due to the noncentral forces. For the BGT potential, the binding energy at normal density ( $k_F=1.52$  F $^{-1}$ ) in the absence of the even tensor force is -2.8 MeV compared with -16.9 MeV for the full potential. This contribution of -14.1 MeV from the tensor force is to be compared with -9.0 MeV determined in second Born approximation by Moszkowski and Scott.<sup>10</sup>

### C. Comparison with the Separation Method of Moszkowski and Scott

Scott and Moszkowski have determined binding energy and density for the BGT potential and for potential 4305 of Gammel and Thaler (see Table I),

TABLE V. Iteration sequences for Brueckner method and for Mohling-Puff approximation as implemented in this paper. Calculations are for BGT potential at  $r_0=1.00$  F. The self-consistent potential  $V(k)$  was averaged between iterations for the Mohling-Puff approximation, improving the convergence of the binding energy sequence to that shown.

Major iteration	Binding energy in MeV	
	Brueckner method	Mohling-Puff approximation
1	-32.963	-2.110
2	-15.720	-15.338
3	-16.936	-17.554
4	-16.887	-17.990
5	-16.892	-18.045
6		-18.033
7		-18.017

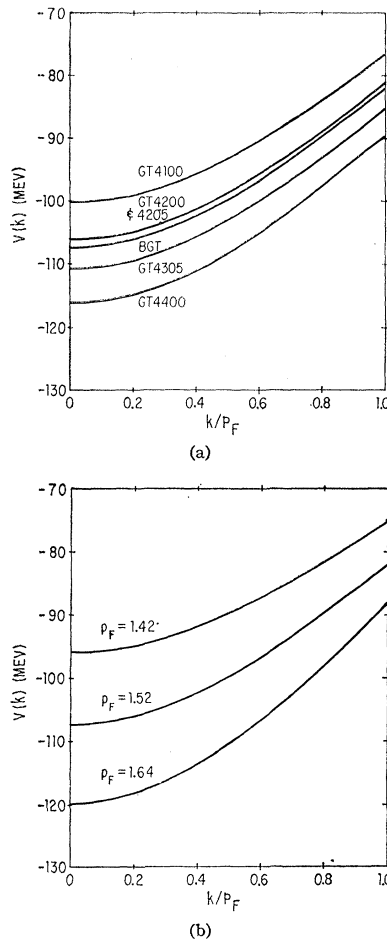


FIG. 6. Variation of self-consistent single-particle potential  $V(k)$  (a) with choice of Gammel-Thaler potentials,<sup>7</sup> at  $r_0 = 1.00$  F; (b) with Fermi momentum,  $p_F$ , using the BGT potential.

using an approximation procedure based on the similarity of the wave function due to the core to that for free scattering. This method is described in detail in their papers,<sup>9,10</sup> and we only give the results here.

They found at normal density binding energies of  $-14.2$  and  $-23.6$  MeV, respectively, for the potentials BGT and GT 4305 (modified to include the BGT triplet-odd parameters). They included contributions from all states with  $l \leq 4$ . Their results for just  $S$ ,  $P$ , and  $D$  waves were  $-13.6$  and  $-22.8$  MeV, respectively. The more accurately determined values obtained by the methods of this paper are  $-16.9$  and  $-21.0$  MeV for the same potentials. In addition, the same calculation fails to obtain saturation for the modified GT 4305 potential, in contrast to our minimum,  $-22.1$  MeV at  $r_0 = 0.91$  F. Their results, and ours, are shown in Fig. 8.

In Table VI we present a breakdown of the contributions to the binding energy for the BGT potential as computed with our code and as reported by Scott and Moszkowski.<sup>10</sup> The contributions of the  $D$  states (and probably of higher states) are given with reasonable

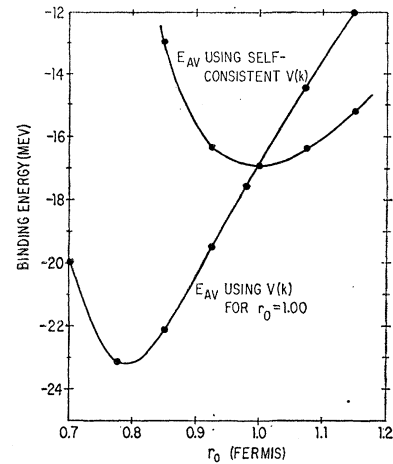


FIG. 7. Binding energy vs  $r_0$  for BGT potential using self-consistent single-particle potential,  $V(k)$ , for  $r_0 = 1.00$  F at all densities.

accuracy by the Moszkowski-Scott method (within 0.5 MeV). However, the  $S$ - and  $P$ -state contributions differ from our values by  $-5.2$  and  $+2.3$  MeV, respectively. A major portion of the differences is probably a consequence of neglecting higher order terms. It should be mentioned that the Moszkowski-Scott method employs a relative momentum approximation for the energy dependence, as we have in this paper. Therefore, their results are more properly compared to our results than to those of BG.

The failure to obtain saturation for GT 4305 is to a considerable extent a consequence of using the Brueckner-Gammel self-consistent  $V(k)$  for the BGT potential instead of a properly self-consistent  $V(k)$ . As we have already shown (Figs. 6 and 7), the dependence of the computed nuclear properties on the self-consistency of the single-particle potential,  $V(k)$ , is very marked.

Kohler<sup>15</sup> and Scott and Moszkowski<sup>16</sup> have reported a "new separation method" which converges more rapidly than the method used to obtain the results above. However, the new method gives less binding for the calculations reported, which would lead to even poorer agreement with our results.

#### D. Comparison with the Mohling-Puff Approximation

As emphasized by Bell, the central element of the nuclear matter theories of Mohling and of Puff is a scattering operator defined by Eq. (1) of reference 11, which differs from Eq. (1.1) as follows:

- (1) The excited state energies,  $E_i^*$ , are replaced by  $p_i^2/2M$ .
- (2) The exclusion principle is ignored for scattering into intermediate states.

<sup>15</sup> S. Kohler, Ann. Phys. (New York) **16**, 375 (1962).

<sup>16</sup> B. L. Scott and S. A. Moszkowski, Nuclear Phys. **29**, 665 (1962).



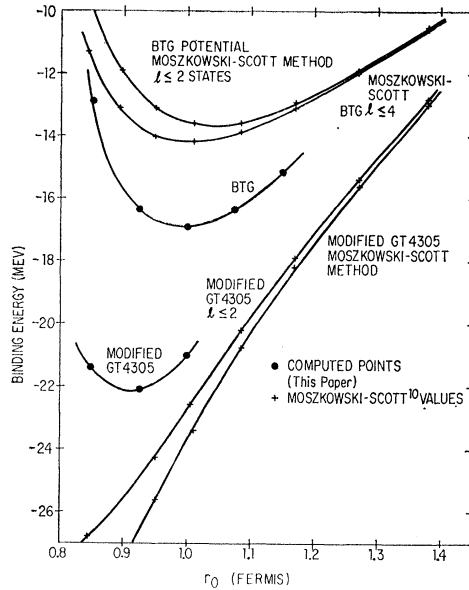


FIG. 8. Binding energy vs  $r_0$  for BGT and modified GT 4305 potentials as computed by Brueckner method (this paper) and by the Moszkowski-Scott method.<sup>10</sup>

The energies  $E_i$  of particles in the Fermi sea are determined as in BG from Eq. (1.2). This approximation method is clearly a large departure from the BG method. Bethe has suggested that the Mohling-Puff approximation may nevertheless be quantitatively accurate, with the corrections arising from the two changes approximately cancelling.

In order to avoid in our calculations the difficulties of a vanishing denominator in Eq. (1.1) on the first major iteration (in which all energies are approximated by kinetic energies), the Pauli exclusion principle was invoked for this iteration only. Because the initial convergence of successive major iterations was very poor (ten iterations for convergence to within  $\pm 0.02$  MeV), we averaged the single-particle potentials between iterations, and obtained the sequence indicated in Table V.

The results of this method are given in Fig. 9. The variation of energy with density is appreciably different for the two methods, with the Mohling-Puff approximation equilibrium values being  $-18.6$  MeV at  $0.90$  F compared to our value of  $-16.9$  MeV at  $1.00$  F for the BGT potential, and similar disagreement for the GT 4400 potential. In both cases, the value of  $r_0$  at the energy minimum is 10% less than our value.

## V. CONCLUSIONS

Our results indicate a definite dependence of the predicted properties of nuclear matter on the choice of phenomenological potential. Although these calculations are not a sufficient criterion for selecting a "best" or "proper" potential, they do emphasize the desirability of further investigation in phenomenological

TABLE VI. Analyses of contributions to binding energy as calculated in this paper and by Moszkowski and Scott (see reference 10). The tensor contribution was calculated by setting  ${}^3V_{T^+}=0$  and computing the binding energy (a) with a single-particle potential  $V(k)$  that is self-consistent with respect to the modified phenomenological potential, and (b) with the single-particle potential  $V(k)$  with which the  $S$ -,  $P$ -, and  $D$ -state contributions were computed. Moszkowski and Scott used a first-order approximation to a self-consistent  $V(k)$  to compute the tensor contribution.

	Brueckner method (this paper)	Moszkowski-Scott method 1st order	2nd order	Total
$S$ states	-38.7	-28.6	-4.9	-33.5
$P$ states	+0.6	-2.3	+0.6	-1.7
$D$ states	-7.5	-7.1	...	-7.1
Total	-45.6	-38.0	-4.3	-42.3
Binding energy	-16.9			-13.6
Tensor contribution				
(a) self-consistent	-14.1			-9.0
(b) with $V(k)$ above	-16.7			

potentials, with particular emphasis on a criterion for uniqueness. The uncertainty in the triplet-even potential does not appear to have been resolved satisfactorily by requiring asymptotic match to the one-meson-exchange potential. The choice of the core radius is also still somewhat arbitrary for those potentials employing a hard core. Determination of the optimum core size from experimental considerations would be very valuable. Gammel and Thaler considered their singlet-even potential to be a unique solution for a Yukawa potential, with  $r_c=0.4$  F, but were unable to differentiate in triplet-even states between cores of 0.3, 0.4, and 0.5 F. Breit and his co-workers<sup>8</sup> state that the employment of hard cores was arbitrary.

Our calculations have shown that the integral equations of the Brueckner theory can be solved by successive approximation. The requirements are that the wave function iteration, which corresponds to successive Born approximations, be carried to at least the equivalent of the third Born approximation for reasonable accuracy

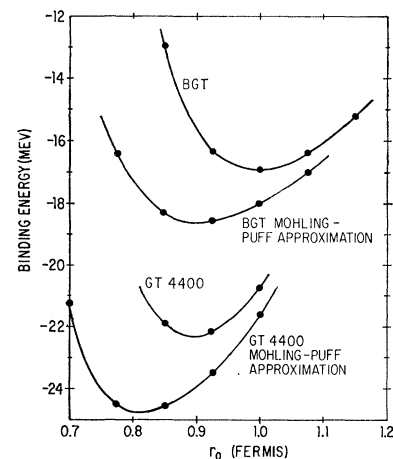


FIG. 9. Binding energy vs  $r_0$  as computed by Brueckner method (this paper) and with the Mohling-Puff approximation (see text).

(+0.5 MeV), and the self-consistent single-particle potentials determined to first order in the  $K$  matrix. The sensitivity of results to the tensor-central force admixture demonstrates the requirement for accurate treatment of the tensor force.

The Moszkowski-Scott separation method does not account for the effects of the tensor potential or the  $S$ - and  $P$ -state contributions to sufficiently high order for accurate results, largely for the reasons stated above. However, the Moszkowski-Scott calculations do give good qualitative and semiquantitative (to second order) results in a simple and intuitively pleasing calculation, presumably for any potential provided the self-consistency requirement is met.

The Mohling and Puff-Martin approximation, as we have employed it, also gives semiquantitative results,

leading to errors in binding energy and equilibrium spacing of about 10%. No appreciable reduction of the computational complexities results from this approximation, so that its utility is questionable.

#### ACKNOWLEDGMENTS

We wish to acknowledge the cooperation and assistance of the computation facilities of the U. S. Navy Electronics Laboratory, San Diego, California (directed by Dr. M. H. Halstead) and of the University of California, San Diego (directed by Dr. C. L. Perry), and we particularly wish to thank Mr. and Mrs. S. W. Porter of NEL for assistance with NELIAC, the compiler used for these calculations. We are also indebted to Dr. John L. Gammel for suggesting a Padé approximant for Eq. (3.2), the Green's function correction.

## Investigation of the Influence of Angular Momentum on Fission Probability

JOHN GILMORE, STANLEY G. THOMPSON, AND I. PERLMAN

*Lawrence Radiation Laboratory, University of California, Berkeley, California*

(Received July 23, 1962)

A nuclear emulsion technique has been used to determine total fission cross sections in the following heavy-ion bombardments: ( $C^{12}+Tm^{169}$ ;  $O^{16}+Ho^{165}$ ), ( $O^{16}+Tm^{169}$ ;  $Ne^{20}+Ho^{165}$ ), ( $C^{12}+Re^{185}$ ;  $O^{16}+Ta^{181}$ ), ( $O^{16}+Re^{185}$ ;  $Ne^{20}+Ta^{181}$ ). Each pair of bombardments resulted in the same compound nucleus, and excitation energies could be made equal in the two cases by adjustment of bombarding energies. The ratio of the fission cross section to a calculated compound-nucleus-formation cross section,  $\sigma_f/\sigma_c$ , was taken as a measure of fission probability in each bombardment. Larger fission probabilities were observed to occur for the systems having greater angular momenta.

**S**TUDIES of heavy-ion-induced nuclear reactions have included a number of investigations of the fission process. One conclusion from these investigations is that fission represents a significant fraction of the total reaction cross section, even for relatively light nuclei. In the bombardment of rhenium with  $N^{14}$  ions, Druin, Polikanov, and Flerov report that fission accounts for about 30% of the reaction cross section at a bombarding energy of 100 MeV.<sup>1</sup> This proportion increases to more than 50% when  $Au^{197}$  and  $Bi^{209}$  are bombarded with heavy ions.

One factor contributing to such high probabilities for fission is that the compound nuclei are neutron deficient, with relatively large values of the fissionability parameter  $Z^2/A$ . High neutron binding energies in these compound nuclei also favor the competition of fission over neutron emission.

Compound nuclei formed in heavy-ion bombardment are further characterized by formation with as much as 100  $\hbar$  of angular momentum. The possibility that

angular momentum may affect fissionability has been discussed by Pik-Pichak.<sup>2</sup> Using the liquid drop model to evaluate the saddle-point deformation and rotational energies, Pik-Pichak showed that the barrier against fission decreases with increasing angular momentum. Calculations of this type have also been performed by Hiskes.<sup>3</sup> Another approach to the evaluation of an angular momentum effect has been taken by Halpern<sup>4</sup> and by Huizenga and Vandenbosch.<sup>5</sup> These authors point out that if an appreciable part of the excitation energy is taken up in rotational motion, the level width for neutron emission becomes small relative to that for fission.

The object of this work was to determine the effect of angular momentum on the probability for fission in heavy-ion bombardment. Pairs of isotopes were bombarded with different heavy ions to give the same

<sup>2</sup> G. A. Pik-Pichak, *Soviet Phys.—JETP* **7**, 238 (1958).

<sup>3</sup> John R. Hiskes, Ph.D. Thesis, University of California Lawrence Radiation Laboratory Report UCRL-9275, 1960 (unpublished).

<sup>4</sup> I. Halpern, *Ann. Rev. Nuclear Sci.* **9**, 245 (1959).

<sup>5</sup> J. R. Huizenga and R. Vandenbosch in *Nuclear Reactions* [North-Holland Publishing Company, Amsterdam, Netherlands (to be published)], Vol. 2.

\* Work done under the auspices of the U. S. Atomic Energy Commission.

<sup>1</sup> V. A. Druin, S. M. Polikanov, and G. N. Flerov, *Soviet Physics—JETP* **5**, 1059 (1957).